Nanoscale

Accepted Manuscript

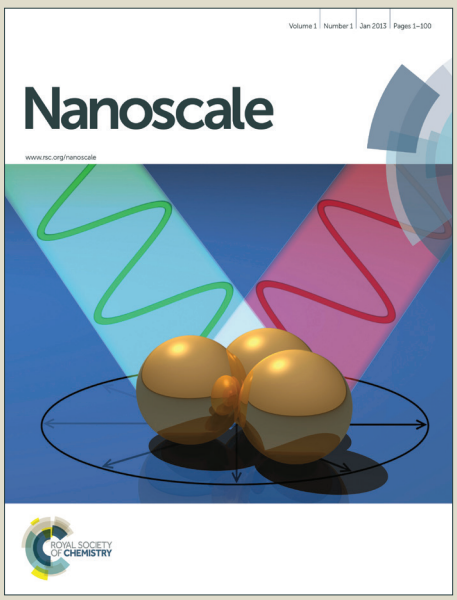

ROYAL SOCIETY OF CHEMISTRY

www.rsc.org/nanoscale

Journal Name

RSCPublishing

ARTICLE

Intelligent Layered Nanoflare: "Lab-on-a-Nanoparticle" for Multiple DNA Logic Gate Operations and Efficient Intracellular Delivery

Cite this: DOI: 10.1039/xoxxoooooox

Received ooth January 2012,
Accepted ooth January 2012

DOI: 10.1039/xoxxoooooox

www.rsc.org/

Bin Yang, Xiao-Bing Zhang,* Li-Ping Kang, Zhi-Mei Huang, Guo-Li Shen, Ru-Qin Yu and Weihong Tan*

DNA strand displacement cascades have been engineered to construct various fascinating DNA circuits. However, their further biological applications are limited by insufficient cellular internalization of naked DNA structures, as well as the separated multicomponent feature. In this work, these problems are addressed through the development of a novel DNA nanodevice, termed intelligent layered nanoflare, which integrates DNA computing at the nanoscale via self-assembly of DNA flares on a single gold nanoparticle. As a "lab-on-a-nanoparticle", the intelligent layered nanoflare could be engineered to perform a variety of Boolean logic gate operations, including three basic logic gates, one three-input AND gate, and two complex logic operations, in a digital, nonleaky way. In addition, the layered nanoflare can serve as a programmable strategy to sequentially tune the size of nanoparticles, as well as a new fingerprint spectrum technique for intelligent multiplex biosensing. More importantly, the nanoflare developed here can also act as a single entity for intracellular DNA logic gate delivery without the need for commercial transfection agents or other auxiliary carriers. By incorporating DNA circuits on nanoparticles, the presented layered nanoflare will broaden the applications of DNA circuits in biological systems and facilitate the development of DNA nanotechnology.

Introduction

Similar to information processing in a computing device, the physiological behavior in cells can orchestrate the continuous input of information and then execute the outputs to precisely control gene expression, enzymatic activity, and interactions in signaling networks.[1] Therefore, sensors with single-input diagnosis are not suitable for processing chemical and biological inputs in such a complex system, even though they have been successfully employed for biosensing in test tubes. Instead, logic gates with the ability to process multiple inputs can solve this problem by integrating these multiple inputs according to a set of predefined rules and, in turn, making decisions with the appropriate responses.[2] In this way, engineering biomolecule-based logic systems could help to control cellular functions and expand the manipulation of biological information through cellular network.[1,3] Among these biomolecule-based computers, DNA-based logic gates and computation are particularly interesting for the construction of biochemical circuits first by the very nature of biological DNA and, second, by such features as easy chemical synthesis and adherence to the highly predictable Watson-Crick complementarity principle.[4,5] Specifically, an approach known as toehold-mediated DNA strand displacement has enabled enzyme-free DNA dynamic devices automated by hybridization alone, inspiring the development of various complex DNA circuits.[5-9]

Because of its negatively charged and hydrophilic features, naked DNA structures cannot easily traverse the cell membrane.[10] As a result, most DNA circuits can only function in test tubes,[4-10] which hampers their potential to interface with biological circuits in vivo. Although several DNA logic gates have been successfully engineered to function in a cellular environment, they required an additional delivery system, such as commercial transfection agents or microinjection for efficient cellular internalization.[11,12] However, insufficient cell delivery, high immunogenicity, harmfulness to living cells, and instability in complex biological environments have limited their further applications in a cellular environment. To overcome these limitations, it is highly desirable to develop another strategy for intracellular delivery of exogenous DNA logic gates, featuring low toxicity and high efficiency. Nonetheless, previous DNA logic gates functioning in the test tube have served as successful proofs of principle in homogeneous solutions. As suggested previously, it may, however, be difficult for them to operate in "stratified" media, such as cellular environments,[13] because the separated moieties of DNA logic gates cannot freely interact with each other in such media. Therefore, it is necessary to develop a nanoscale platform to integrate DNA circuits into a single entity. Creating complex, multifunctional devices on a single nanoparticle platform can also be beneficial in achieving increased logic complexity and promoting the application of logic gates in DNA nanotechnology.

A new class of probe developed for bioanalysis and termed nanoflare has been described as "consisting of a gold

nanoparticle (AuNP) core, surrounded by a dense monolayer of oligonucleotides able to detect mRNA with single-cell resolution."[14] The nanoflare itself possesses a set of unique properties that make it a potentially excellent intracellular DNA logic gate delivery agent, namely, dense functionalization for large charge, high uptake dose into diverse cell types without transfection agents, high stability in biological environments, no observable toxicity, and low immunogenicity.[15-17] Surface energy transfer (SET), the mechanism providing energy transfer in the nanoflare, can extend the usable length scale for fluorescence detection up to 70 nm.[18,19] Thus, the AuNPs-based nanoflare has the potential to allow the construction of complex DNA molecular switches on its surface, which is the foundation for building complex logic systems. In addition, the AuNPs are able to simultaneously quench various dyes with different emission frequencies from the visible range to near-IR.[20] Therefore, AuNPs-based nanoflares can be used to engineer complex logic systems in which multiple fluorescence signals need to be outputted. Combining the advantages of AuNPs-based nanoflares, as mentioned above, with the rich capability of the layered DNA nanostructure for scaling up digital circuitry,[5-9] we sought to develop an intelligent layered nanoflare to engineer complex logic systems on a single AuNP and further use it as a single entity to efficiently deliver an exogenous DNA logic gate into living cells.

Experimental

Materials and instrumentation

Hydrogen tetrachloroaurate(III) tetrahydrate, FSN, adenosine 5-triphosphate (ATP), guanosine 5-triphosphate (GTP), and other chemicals were obtained from Sigma-Aldrich (China). The molecular formula of FSN is $F(CF_2CF_2)_{3-8}CH_2CH_2O(CH_2CH_2O)_xH$, as indicated by the product manual. DNA oligonucleotides were synthesized and HPLC-purified by Sangon Biotechnology Co., Ltd (Shanghai, China). The sequences of the involved oligonucleotides are listed in Table S1 (Electronic Supplementary Information). Water used in all experiments was doubly distilled from a Milli-Q system (Millipore, USA). Following the literature procedure, AuNPs with average diameters of 13 nm were prepared by the reduction of $HAuCl_4$ with citrate.[21]

Fluorescence measurements were carried out at 25 °C on a FluoroMax-4 spectrofluorometer (Horiba Jobin Yvon, France). The absorption spectra of AuNPs were measured on a UV-2450 spectrophotometer (Shimadzu). Dynamic light scattering (DLS) was determined on a Zeta Sizer Nano ZS. Transmission electron microscopy (TEM) images were obtained at an accelerating voltage of 100 kV using a JEOL1400 model.

Logic gate and nanoflare formation

TAE/Mg^{2+} buffer (0.04 M Tris-acetate, 1 mM EDTA, 12.5 mM Mg acetate, pH 8.3) was used for all reactions, including fluorescence experiments and gel electrophoresis analysis. Logic gate formation: Gates were formed via slow annealing, in which the mixture solution was heated to 95 °C and then slowly cooled down. Taking the AND gate as an example, 2 μL 100 μM E-SH, 2.5 μL 100 μM F_f, and 3 μL 100 μM G were added to 94 μL TAE/Mg^{2+} buffer, and the mixture was annealed as described above. Nanoflare formation: To 500 μL 3 nM of the FSN-capped AuNPs, 50 μL 5 M NaCl and the annealed gate solution were added. The solution was allowed to incubate at room temperature overnight. Then the solution was centrifuged (12,500 rcf, 10 min, 4 °C) and washed three times using 500 μL phosphate buffer saline (PBS) (137 mM NaCl, 10 mM phosphate, 2.7 mM KCl, pH 7.4, Hyclone). Finally, the nanoflare was resuspended in 500 μL TAE/Mg^{2+} buffer and stored at 4 °C.

Fluorescence kinetics measurements

All the fluorescence kinetics experiments were measured with each reaction volume of 100 μl at 25 °C. The fluorescence of FAM-labeled green flare was excited at 480 nm and detected at 520 nm; the fluorescence of TAMRA-labeled red flare was excited at 559 nm and detected at 583 nm; the fluorescence of Rox-labeled pink flare was excited at 588 nm and detected at 608 nm. Both the excited and emission slits were set to be 2.0 nm. Taking the AND gate as an example, 90 μl 3 nM nanoflare was added to a fluorescence cuvette, and its initial fluorescence signal was recorded for 500 seconds. Then, 5 μl 6 μM G_{in} or F_{in} was introduced using a microsyringe and quickly stirred. The sample was incubated until the fluorescence signal reached equilibrium and finally recorded for another 500 seconds.

Gel electrophoresis analysis

The 2% agarose gels were prepared using TBE buffer (1×), and a volume of 10 μL of 3 nM nanoflare with loading buffer (1×) was added to each lane. Then agarose gels were run at 110 V for 40 min and visualized over white light using a Samsung digital camera.

Cell culture

Cell line HeLa was obtained from the American Type Culture Collection (Manassas, VA). HeLa cells were cultured in RPMI 1640 medium (GIBCO), which was supplemented with 10% fetal bovine serum (FBS) (heat inactivated, GIBCO) and 0.5 mg/mL penicillin-streptomycin (Cellgro) at 37 °C in a humid atmosphere with 5% CO_2. Dulbecco's Phosphate-Buffered Saline (D-PBS, 1.47 mM KH_2PO_4, 8.06 mM Na_2HPO_4, 137.93 mM NaCl, 2.67 mM KCl) was purchased from Hyclone. The cell density was measured using a hemocytometer prior to seeding.

Confocal microscopy imaging

1 x 10^5 HeLa cells were seeded in a poly-d-lysine-coated 35 mm glass bottom dish and incubated in 1mL cell medium for 24 h. After replacing cell medium, cells were incubated with 2 nM nanoflares for 5 h. Then cells were prepared by rinsing with D-PBS, trypsinization, and resuspension in D-PBS. Cellular fluorescent images were collected on the FV500-IX81 confocal microscope (Olympus America Inc., Melville, NY) with 100x oil immersion objective (NA=1.40,Olympus, Melville, NY) and Fluoview analysis software. Excitation wavelength and emission filters were set to 588 nm and 608 ± 10 nm.

Results and discussion

AND logic gate

The intelligent layered nanoflare was prepared by assembling the layered DNA nanostructure on citrate-capped 13 nm AuNPs via gold–thiol bond formation (Figure S1 in Electronic Supplementary Information). It was realized in a one-pot way using a fluorosurfactant-assisted procedure,[21] and the surface density of DNA on AuNPs was determined to be about 60

strands/particle (see Figure S2 in Electronic Supplementary Information). Figure 1A depicts the design of the nanoflare for the AND logic gate, which is based on two cascades of toehold-mediated DNA strand displacement.[6] After the first input G_{in} binds to its toehold on the outermost layer of the nanoflare, it displaces the oligonucleotide G via three-way branch migration, exposing the toehold on the inner layer for subsequent input F_{in}. Following a similar process, the concomitant release of green flare F_f can be detected as a corresponding increase in green fluorescence (Figure 1B). By caging toehold regions in this layered DNA structure, the green flare F_f (output = 1) can be released only if both inputs G_{in} and F_{in} are present (input=1, 1). As indicated in the time-dependent fluorescence changes (Figure 1B), another mechanism, termed "toehold exchange,"[22] when coupled with G_{in}-6 and F_{in} as the two inputs, could also successfully function as an AND logic gate. The absence of any correlation between the sequences of the two inputs G_{in}-6 and F_{in} in our system allows flexible choice of input combinations, providing a more suitable approach for the rational design of dynamic DNA nanodevices and sensors.

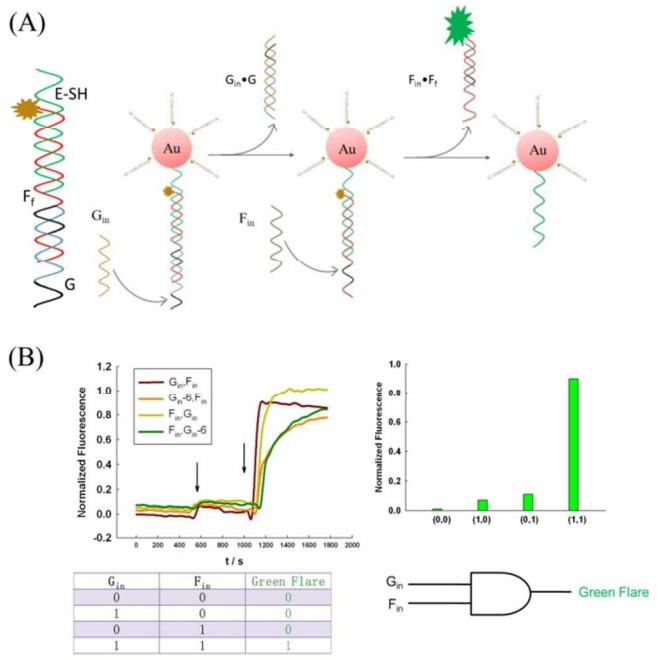

G_{in}	F_{in}	Green Flare
0	0	0
1	0	0
0	1	0
1	1	1

Figure 1 (A) Schematic representation of the AND gate based on the intelligent layered nanoflare (Left: the enlarged picture of the DNA nanostructure on gold nanoparticle). (B) Time-dependent fluorescence changes, bar diagram, truth table, and logic scheme for the AND gate.

The AuNPs in this layered nanoflare system have several unique advantages over the organic quencher employed in previous research.[6] First, a cooperative property arising from the dense monolayer of DNA on the nanoparticle surface can increase the hybridization rate, thus allowing fast logic gate operation.[23] Second, high absorption efficiency makes AuNPs an ideal quencher to obtain significant fluorescent change for a logic switch.[18,19] Third, only the centrifugation procedure can effectively purify the logic gate to decrease signal leaking, while in previous research, the gates require a cumbersome purification process by gel electrophoresis.[5-7]

To verify AND gate operation in Figure 1 A, the size change of the layered nanoflare was investigated by dynamic light scattering (DLS) (Figure 2A). After introducing the first input, G_{in}, a substantial decrease (~10 nm) of the average hydrodynamic diameter was observed by the stripping of the outside layer G. The subsequent addition of the second input, F_{in}, then separated the inner layer flare, F_f, from the AuNPs, further decreasing the hydrodynamic diameter (~6 nm) of the nanoflare. Interestingly, this double-response AND logic gate can also serve as a novel programmable strategy to sequentially tune the size of nanoparticles via customized DNA displacement alone.[24]

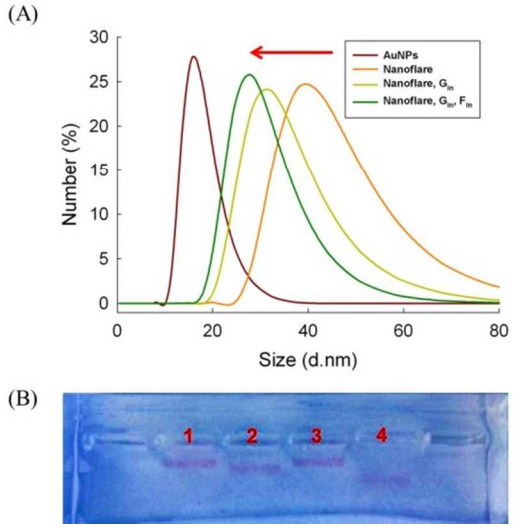

Figure 2 (A) Hydrodynamic sizes of the nanoflare for the AND gate determined by DLS analysis; (B) Gel demonstrating the AND gate operation for each possible input combination: lane 1, none; lane 2, G_{in}; lane 3, F_{in}; lane 4, G_{in} and F_{in}.

To further verify whether the nanoflare proceeded as designed, a gel electrophoresis experiment was carried out (Figure 2 B). After the addition of input G_{in}, a new band appeared in lane 2 with slightly faster mobility than that in lane 1, indicating the successful stripping of the outside layer of the nanoflare. In contrast, the input F_{in} alone (lane 3, Figure 2 B) caused no change in band shift compared to the initial nanoflare (lane 1, Figure 2 B) as a result of the caging of the toehold region by the outer layer G, which is also a key working principle underlying the design of this AND gate. In the presence of inputs G_{in} and F_{in} (lane 4, Figure 2 B), the band of the nanoflare moved most rapidly, confirming the full stripping of both layers. Both DLS and gel electrophoresis results were in good agreement with those obtained with fluorescence measurements (Figure 1 B), which robustly confirmed the mechanism with the two cascades of toehold-mediated DNA strand displacement.

Basic logic gates

To complete the basic Boolean logic gate operations, we also sought to construct a nanoflare-based OR gate using a similar design strategy. The nanoflare for the OR gate was engineered by assembling a mixed monolayer of flares for the inputs G_{in} and F_{in} on a single AuNP, while each red flare was labeled with the same TAMRA dye (Figure 3 A). In this way, the addition of either input, G_{in} or F_{in}, displaces its respective recognition oligonucleotide to liberate the red flare. Thus, the nanoflare responds with an obvious increase in red fluorescence signal (Figure 3 B). The NOT gate was also successfully constructed based on the nanoflare (Figure 4 A). In this case, a pink flare hybridized with its complementary oligonucleotide G on the

outer layer of the nanoflare. The addition of the input G_{in} removed the outside layer G, changing the stiff double-stranded oligonucleotide into a flexible single-stranded one.[25] Based on the distance-dependent fluorescence quenching ability of AuNPs, this process decreased the fluorescence signal (about 32.6% signal decrease) to successfully construct the NOT gate (Figure 4 B). All complex logic functions can be engineered using the set of basic functions, including AND, OR, and NOT.[26] As such, these layered nanoflares have the potential to allow for the construction of combinatorial logic circuitry with more sophisticated information processing ability, as discussed below.

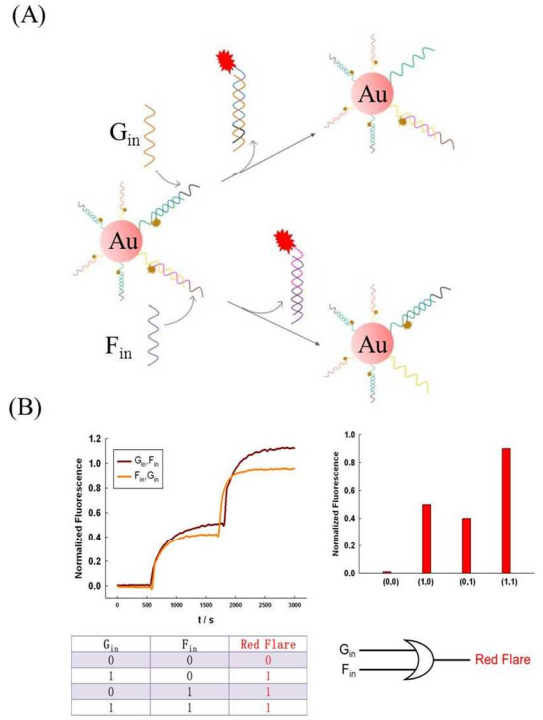

Figure 3 (A) Schematic representation of the OR gate. (B) Time-dependent fluorescence changes, bar diagram, truth table, and logic scheme for the OR gate.

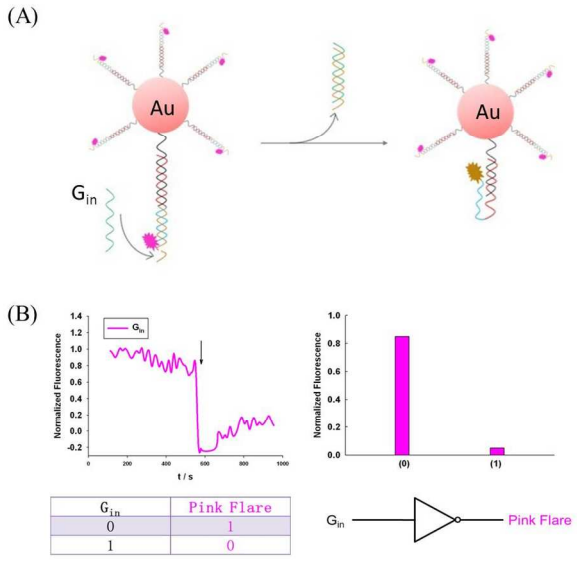

Figure 4 (A) Schematic representation of the NOT gate. (B) Time-dependent fluorescence changes, bar diagram, truth table, and logic scheme for the NOT gate.

Three-input AND gate

Based on the specific and selective binding capability of aptamer molecules, it is also desirable to develop an aptamer-based layered nanoflare for logic gate operation. As shown in Figure 5 A, a three-input AND gate was designed simply by tethering a DNA aptamer as an additional layer to the nanoflare for the two-input AND gate. In the absence of ATP, the presence of both G_{in} and F_{in} inputs could not activate this three-layered nanoflare because of the reliable caging of the toehold region by the ATP-targeting aptamer (Figure 5 B, brown line). In contrast, an obvious fluorescent signal was observed after the subsequent addition of 1mM ATP, suggesting the successful construction of a three-input AND gate involving a small biomolecule as an input. The proposed logic gate also maintained the high selectivity of the aptamer for ATP because 1 mM GTP induced only a negligible change of fluorescence signal (Figure 5 B, green line). Since the targets of aptamers range from small molecules and metal ions to proteins, biological cells, and tissues,[27,28] the introduction of aptamers provides more possible choice of inputs for DNA computation, thus resulting in its wider application in the biological system.

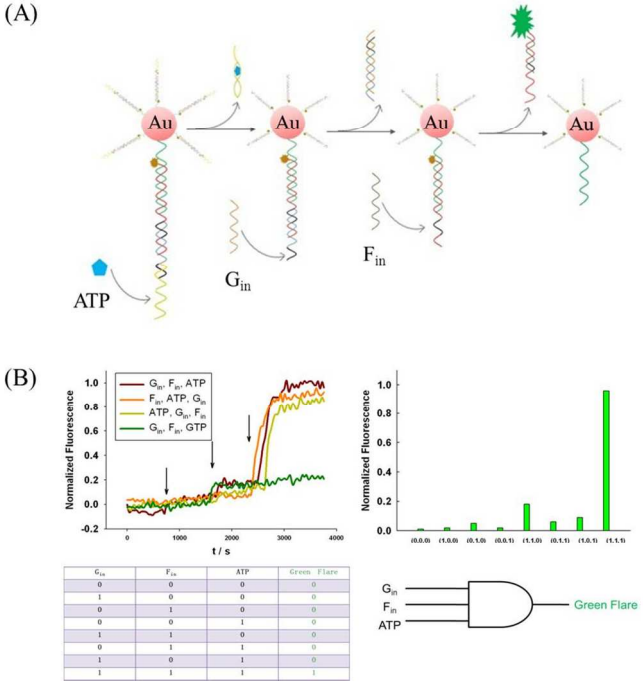

Figure 5 (A) Schematic representation of the three-input AND gate. (B) Time-dependent fluorescence changes, bar diagram, truth table, and logic scheme for the three-input AND gate.

Complex multiple logic systems

After implementing the basic Boolean logic gates, the layered nanoflare was then designed to activate a complex multiple logic system 1, combining AND, YES and NOT-INHIBIT operations. This was achieved by simply modifying three fluorophores on different sites of the two-layered dsDNA structure (Figure 6 A). Each of the flares having a different fluorophore served as the output of the corresponding operation, i.e., green flare = AND; red flare = YES; and pink

flare = NOT-INHIBIT (Figure 6 B). The response process of the AND logic function is the same as that of the nanoflare for the two-input AND gate, while the YES function is activated in a manner similar to that of the OR gate in Figure 3 A, but on the outermost layer of the nanoflare. The NOT-INHIBIT function, as indicated by a pink flare (Figure S3 in Electronic Supplementary Information), corresponded to a true value in the presence of all possible sets of inputs, except input G_{in} alone. To activate the NOT-INHIBIT operation, either the absence or presence of both inputs will separate the pink flare from the AuNP, either by the stiff structure of dsDNA, or by fully stripping the pink flare, respectively (Figure S3 in Electronic Supplementary Information).

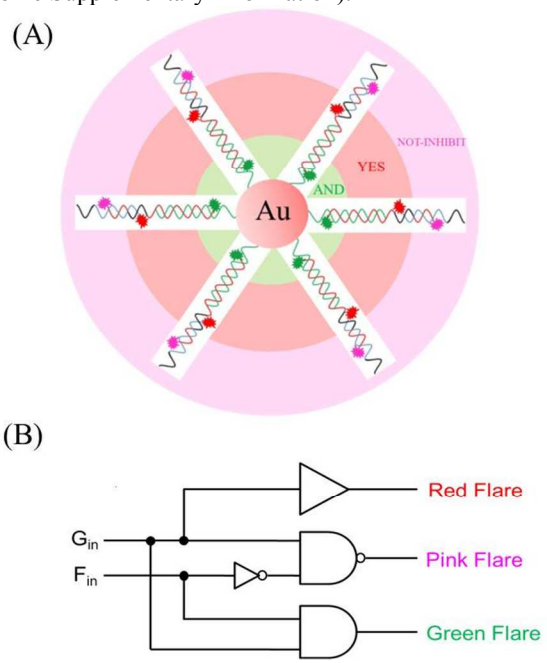

Figure 6 (A) Schematic representation and (B) logic scheme of the multiple logic system 1.

To design a multiple DNA logic system in a more rational way, multiple logic system 2 was developed to accommodate more customized needs by assembling mixed monolayers of dsDNA flares on a single AuNP (Figure 7 A). The DNA sequences and logic operations are similar to the AND, OR and NOT logic gates mentioned above, but they are assembled on a single AuNP (Figure 7 B), instead of different ones (Figure 1, 3, and 4). From the truth table in Figure S4 (Electronic Supplementary Information), the possible input combinations can also be digitally coded with the output of different flares. That is, (0, 0), (0, 1) (1, 0) and (1, 1) were coded as (0, 0, 1), (0, 1, 0), (0, 1, 1) and (1, 1, 0), respectively. In this way, the multiple DNA logic system could also serve as a novel fingerprint spectrum technique for intelligent multiplex biosensing.[29]

In the two multiple logic systems, the same set of two inputs can perform several logic operations in a rapid and parallel manner via a simple self-assembly approach. This system is easier to design than the unimolecular platform.[230] It is also smaller than the assembly system on bulk materials[31] and responds more rapidly than multilayer circuit design.[5,7] The nanoflare is a "lab-on-a-nanoparticle" prototype, since it can integrate numerous independent logic gate components into a single nanoparticle and output a clever result by simultaneously processing information of several signal channels.[32] Therefore, these layered nanoflares with versatile operations provide a new route to scale up DNA computing circuits and to design complex DNA nanodevices.

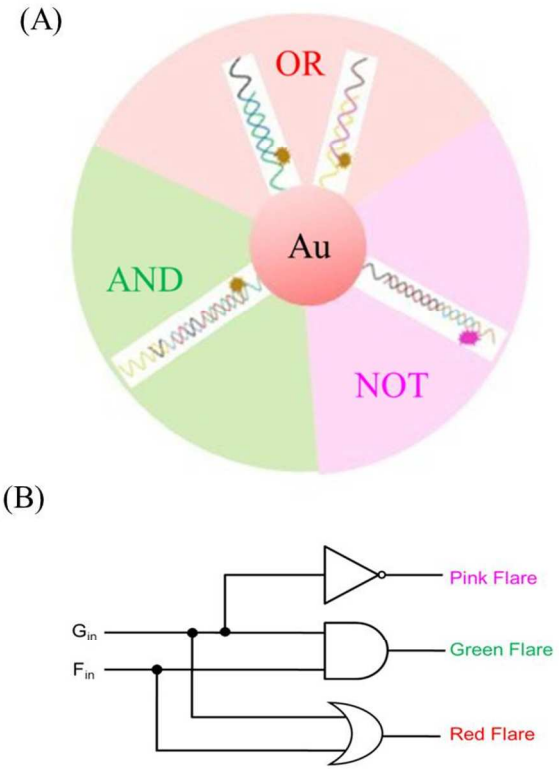

Figure 7 (A) Schematic representation and (B) logic scheme of the multiple logic system 2.

Intracellular Delivery

To demonstrate the potential of the intelligent layered nanoflare for use as a reliable platform for effective delivery of DNA logic gates into a cellular environment, we performed cell culture experiments. By incubating the nanoflare with HeLa cells, its cellular uptake efficiency was characterized by confocal imaging. After incubation in cell medium for 5 h, the resulting HeLa cells exhibited strong pink fluorescence in the cytoplasm (Figure S5 in Electronic Supplementary Information), indicating the excellent internalization of the nanoflare. In this way, the high cellular uptake ability and good biocompatibility of the AuNPs make the nanoflare a better choice for intracellular DNA logic gate delivery than commercial transfection agents or the use of microinjection. In addition, the innovative single nanoparticle element avoids reliance on gene transcription to perform DNA computation.[33]

Conclusions

In conclusion, we have developed a novel DNA nanodevice, termed intelligent layered nanoflare, via self-assembly of layered DNA nanostructure on a single AuNP to increase the complexity of logic gate circuitry beyond basic Boolean operations. Combining the multiple assembly feature of AuNPs, the unique quenching ability for various dyes, and the reliability of this layered DNA structure, the layered nanoflare presented here holds significant potential for the development of more complex DNA computing circuits on just a single nanoparticle. Moreover, the intelligent layered nanoflare has

been successfully designed to deliver DNA logic gates into living cells. Thus, the intelligent layered nanoflare can be used as "lab-on-a-nanoparticle" for the construction of DNA computers and intracellular delivery. As such, this intelligent layered nanoflare can serve as a single entity to expand the potential of DNA logic systems for biological applications, as well as provide a novel strategy for building up complex DNA nanodevices.

Acknowledgements

This work was supported by the National Key Scientific Program of China (2011CB911000), NSFC (Grants J1210040, 21325520, 20975034, 21177036, 21275044), the Foundation for Innovative Research Groups of NSFC (Grant 21221003), the National Key Natural Science Foundation of China (21135001), National Instrumentation Program (2011YQ030124), the Ministry of Education of China (20100161110011), and the Hunan Provincial Natural Science Foundation (Grant 11JJ1002).

Notes and references

Molecular Science and Biomedicine Laboratory, State Key Laboratory of Chemo/Biosensing and Chemometrics, College of Chemistry and Chemical Engineering, College of Biology, Collaborative Innovation Center for Chemistry and Molecular Medicine, Hunan University, Changsha 410082 (P.R. China) Fax: (+ 86)731-88821848 E-mail: xbzhang@hnu.cn; tan@chem.ufl.edu.

Electronic Supplementary Information (ESI) available: additional figures (Table S1, Fig. S1 – S2). See DOI: 10.1039/b000000x/

1 T. Miyamoto, S. Razavi, R. DeRose, T. Inoue, *ACS Synth. Biol.* 2012, **2,** 72.
2 M. Win, C. Smolke, *Science* 2008, **322**, 456.
3 J. Anderson, C. Voigt, A. Arkin, *Mol. Syst. Biol.* 2007, **3**, 133.
4 J. Li, X. Jia, D. Li, J. Ren, Y. Han, Y. Xia, E. Wang, *Nanoscale* 2013,**5**, 6131.
5 L. Qian, E. Winfree, *Science* 2011, **332**, 1196.
6 G. Seelig, D. Soloveichik, D. Y. Zhang, E. Winfree, *Science* 2006, **314**, 1585.
7 L. Qian, E. Winfree, J. Bruck, *Nature* 2011, **475**, 368.
8 J. Zhu, L. Zhang, T. Li, S. Dong, E. Wang, *Adv. Mater.* 2013, **25**, 2440.
9 D. Han, Z. Zhu, C. Wu, L. Peng, L. Zhou, B. Gulbakan, G. Zhu, K. Williams, W .Tan, *J. Am. Chem. Soc.* 2012, **134**, 20797.
10 O. Boussif, F. Lezoualc'h, M. Zanta, M. Mergny, D. Scherman, B. Demeneix, J. Behr, *Proc. Natl. Acad. Sci.* 1995, **92**, 7297.
11 M. Kahan-Hanum, Y. Douek, R. Adar, E. Shapiro, *Sci. Rep.* 2013, **3**, 1535.
12 J. Hemphill, A. Deiters, *J. Am. Chem. Soc.* 2013, **135**, 10512.
13 B. Kowalczyk, D. A. Walker, S. Soh, B. A. Grzybowski, *Angew. Chem. Int. Ed.* 2010, **49**, 5737.
14 D. S. Seferos, D. A. Giljohann, H. D. Hill, A. E. Prigodich, C. A. Mirkin, *J. Am. Chem. Soc.* 2007, **129**, 15477.
15 A. E. Prigodich, P. S. Randeria, W. E. Briley, N. J. Kim, W. L. Daniel, D. A. Giljohann, C. A. Mirkin, *Anal. Chem.* 2012, **84**, 2062.
16 N. Li, C. Chang, W. Pan, B. Tan, *Angew. Chem. Int. Ed.* 2012, **51**, 7426.
17 A. E. Prigodich, D. S. Seferos, M. D. Massich, D. A. Giljohann, B. C. Lane, C. A. Mirkin, *ACS Nano*. 2009, **3**, 2143.
18 P. C. Ray, A. Fortner, G. K. Darbha, *J. Phys. Chem. B* 2006, *110*, 20745.
19 A. Heuer-Jungemann, P. K. Harimech, T. Brown, A. G. Kanaras, *Nanoscale*, 2013, **5**, 9503.
20 E. Dulkeith, M. Ringler, T. A. Klar, J. Feldmann, A. M. Javier, W. J. Parak, *Nano Lett.* 2005, **5**, 585.
21 Y. Zu, Z. Gao, *Anal. Chem.* 2012, **81**, 8523.
22 D. Y. Zhang, A. J. Turberfield, B. Yurke, E. Winfree, *Science* 2007, **318**, 1121.
23 A. E. Prigodich, O. Lee, W. L. Daniel, D. S. Seferos, G. C. Schatz, C. A. Mirkin, *J. Am. Chem. Soc.* 2010, **132**, 10638.
24 T. Zhou, P. Chen, L. Niu, J. Jin, D. Liang, Z. Li, Z. Yang, D. Liu, *Angew. Chem. Int. Ed.* 2012, **51**, 11271.
25 Y. Krishnan, F. C. Simmel, *Angew. Chem. Int. Ed.* 2011, **50**, 3124.
26 K. Szacilowski, *Chem. Rev.* 2008, **50**, 3481.
27 S. D. Jayasena, *Clin. Chem.* 1999, **45**, 1628.
28 Y. Xing, Z. Yang, D. Liu, *Angew. Chem. Int. Ed.* 2011, **50**, 11934.
29 J. Song, J. Zhang, F. Lv, Y. Cheng, B. Wang, L. Feng, L. Liu, S. Wang, *Angew. Chem. Int. Ed.* 2013, **53**, 13020.
30 D. C. Magri, M. Fava, C. J. Mallia, *Chem. Commun.* 2014, **50**, 1009.
31 N. H. Voelcker, K. M. Guckian, A. Saghatelian, M. R. Ghadiri, *small* 2008, **4**, 427.
32 D. C. Magri, G. J. Brown, G. D. McClean, A. P. de Silva, *J. Am. Chem. Soc.* 2006, **128**, 4950.
33 J. Bonnet, P. Yin, M. Ortiz, P. Subsoontorn, D. Endy, *Science* 2013, **340**, 599.

